

AD-A096 309

PENNSYLVANIA STATE UNIV UNIVERSITY PARK DEPT OF MATE--ETC F/6 13/8
HYDROGEN ABSORPTION DURING ELECTRODEPOSITION AND HYDROGEN CHARG--ETC(U)
FEB 81 M ZAMANZADEH, A ALLAM, C KATO, B ATEYA N00014-75-C-0264
TR-16 NL

UNCLASSIFIED

[] []
ADA
C0602 W



END
DATE
FILMED
A-81
DTIC

COLLEGE OF EARTH AND MINERAL SCIENCES

DEPARTMENT OF MATERIALS SCIENCE
METALLURGY SECTION

TECHNICAL REPORT NO. 16

to

OFFICE OF NAVAL RESEARCH
Contract No. N000-14-75-C-0264

HYDROGEN ABSORPTION DURING ELECTRODEPOSITION
AND HYDROGEN CHARGING OF Sn AND Cd COATINGS ON IRON

M. Zamanzadeh,⁺ A. Allam,[†] C. Kato, B. Ateya[†] and H. W. Pickering

Department of Materials Science and Engineering
The Pennsylvania State University
University Park, Pennsylvania 16802

Reproduction in whole or in part is permitted for any purpose of the
United States Government. Distribution of this document is unlimited.

**The Pennsylvania
State University
University Park,
Pennsylvania**



81 3 13 044

AD A U 96309

FILE COPY

II

12

THE PENNSYLVANIA STATE UNIVERSITY

College of Earth and Mineral Sciences

UNDERGRADUATE PROGRAMS OF STUDY

Ceramic Science and Engineering, Earth Sciences, Geography, Geosciences, Metallurgy, Meteorology, Mineral Economics, Mining Engineering, Petroleum and Natural Gas Engineering, and Polymer Science.

GRADUATE PROGRAMS AND FIELDS OF RESEARCH

Ceramic Science, Fuel Science, Geochemistry and Mineralogy, Geography, Geology, Geophysics, Metallurgy, Meteorology, Mineral Economics, Mineral Processing, Mining Engineering, Petroleum and Natural Gas Engineering, and Polymer Science.

UNIVERSITY-WIDE INTERDISCIPLINARY GRADUATE PROGRAMS INVOLVING E&MS FACULTY AND STUDENTS

Earth Sciences, Ecology, Environmental Pollution Control Engineering, Mineral Engineering Management, Operations Research, Regional Planning, and Solid State Science.

ASSOCIATE DEGREE PROGRAMS

Metallurgical Engineering Technology and Mining Technology.

INTERDISCIPLINARY RESEARCH GROUPS WITHIN THE COLLEGE

Coal Research Section, Mineral Conservation Section, Ore Deposits Research Section, and Mining and Mineral Resources Research Institute.

ANALYTICAL AND STRUCTURE STUDIES

Classical chemical analysis of metals and silicate and carbonate rocks; X-ray crystallography; electron microscopy and diffraction; electron microprobe analysis; atomic absorption analysis; spectrochemical analysis.

HYDROGEN ABSORPTION DURING ELECTRODEPOSITION
AND HYDROGEN CHARGING OF Sn AND Cd COATINGS ON IRON

M. Zamanzadeh,[†] A. Allam,[†] C. Kato, B. Ateya[†] and H. W. Pickering

Department of Materials Science and Engineering
The Pennsylvania State University
University Park, Pennsylvania 16802

[†]current address: P.O. Box 98-529, Tajrish, Tehran, Iran

[†]permanent address: Chemistry Department, Cairo University, Cairo, Egypt.

Application For

A

INTRODUCTION

The problem of hydrogen embrittlement of iron base alloys is now well recognized and serious efforts are underway to understand the relevant factors and to prevent or control its incidence. Metallic coatings have frequently been used to minimize the extent of hydrogen uptake by an alloy (a brief review is given in reference [1]). More recently, an alternative method of decreasing hydrogen absorption has been proposed and evaluated (1-3). More severe charging conditions are usually encountered when the source of hydrogen is an aqueous rather than gaseous phase, since a very large fugacity of hydrogen is easily reached by a fairly low hydrogen charging current [4,5]. Such a current is much less than the corrosion current of iron in an acid media and is comparable to that in neutral and alkaline media

During electroplating, hydrogen may be discharged and enter the steel. Very low concentrations of hydrogen, \sim 1ppm, are sufficient to cause degradation of steel, which may be manifested in any of a number of ways such as reduced ductility [6], reduced toughness [7], brittle fracture [8], or stress-corrosion cracking [9]. Different types of heat treatment are usually employed to reduce the hydrogen content in electroplated parts, although heat treatment does not always give good results [10,11]. It is of great interest to use plating baths which introduce little hydrogen into the steel and consequently do not cause embrittlement, and also give a deposit which itself has a low tendency to absorb hydrogen and is a good barrier to hydrogen permeation. Investigations have so far concentrated on cadmium plating baths [12,13], with less attention focused on tin plating baths [14].

Both Sn and Cd appear to have a low permeability [15,16] for hydrogen. Both also are considerably less catalytic than most other metals, including iron, for the hydrogen evolution reaction. Thus, they do not promote corrosion

of the base metal (as do, for example, noble metal coatings) when the base metal is exposed locally.

THEORETICAL

Of the two approaches to decreasing hydrogen absorption, one is based on catalyzing the hydrogen evolution reaction (h.e.r.) by distributing, even sparingly, over the surface a metal with a high exchange current density for the h.e.r. [1-3]. The other is the barrier effect which becomes a factor as the thickness of a dense, continuous coating, which has a low hydrogen solubility and/or diffusivity, increases.

Catalytic Mechanism. The effectiveness of different substrates for promoting the h.e.r. may be described in terms of its exchange current density, i_0 , on these different substrates. When the transfer coefficient is the same on different substrates, the rate, i , of the h.e.r., is simply in the ratio of its exchange current density on these substrates. A deposit with a higher i_0 than the substrate, therefore, provides for a lower average overpotential η on the composite surface for a given charging current I , Fig. 1.[†] This fact may be used to advantage for decreasing hydrogen absorption by the substrate. This occurs for certain mechanisms of hydrogen absorption in which the coverage, and hence the absorption, of hydrogen is a function of the overpotential. In the limiting case of a small amount of deposit, absorption directly via the deposit is very small and can be neglected. For large amounts of deposit the situation will vary depending on the mechanism of hydrogen evolution, and the permeability of hydrogen in the deposit.

In the case of iron the relation between hydrogen coverage, θ , and the overpotential at low coverages is [5],

[†]The change in area of substrate 1 is appropriately neglected when the area of substrate 2 is much smaller than that of substrate 1 and/or $(i_0)_2 \gg (i_0)_1$.

$$\theta = A e^{-\beta n F / 2 R T}$$

where k_2 is the rate coefficient of the hydrogen recombination reaction, β is the symmetry factor of the activation barrier for discharge, and F , R and T have their usual meanings. In the limiting case of a sparse deposit of higher i_0 than the substrate, Eq. (1) may be applied to the composite substrate-deposit surface (Fig. 1).

Thus, a decrease in overpotential due to a deposit of higher i_0 results in a decrease in the hydrogen coverage on the iron surface. It follows that the solubility of hydrogen in the Fe in equilibrium with the coverage also decreases, and then so also does the permeation of hydrogen. Since this catalytic approach for lowering hydrogen uptake from electrolytic solutions is a function of the mechanism of the h.e.r., its effectiveness will vary from metal to metal and even for the same metal under different electrolytic conditions. Thus, the explicit form of the dependency of θ on η will depend on the details of the h.e.r. just as equation (1) applies for the coupled discharge-recombination mechanism of hydrogen evolution. This model is supported by experimental results for pt electrodeposits on iron [1] and for pt-implanted Fe [3]. Both of these iron - platinum composite surfaces cause a significant decrease in the overpotential at constant current and also in the coverage, solubility and permeation of hydrogen.

Barrier Mechanism. A low permeability of hydrogen in the coating requires that a dense coating forms with a low solubility, S , and/or diffusivity, D , for hydrogen. Some indication as to how good a material may be as a barrier can be obtained by comparing either or both of these quantities. Solubility data, however, are sparse at ambient and moderately elevated temperatures; diffusivity data are only somewhat more available. Hydrogen solubility is dependent on the electrolytic charging conditions whereas

diffusivity is not. For coatings to be effective barriers, they need to also be continuous, relatively thick and impervious, and stable in the environment much like protective scales on metals. Then, there will be an appreciable time lapse, even for thin layers, before the activity (concentration) of hydrogen at the coating/substrate interface rises appreciably, or in the limit approaches that which exists in the environment.

The barrier effect, however, does not function independently of the catalytic effect, since the hydrogen charging (evolution) reaction occurs on the coating surface. Thus, the selection of a coating from several metals with equivalent barrier characteristics may come down to a choice based on their catalytic nature for the hydrogen evolution reaction, as discussed above. Thus, choosing a coating with a high exchange current density could further decrease hydrogen uptake. A higher hydrogen evolution rate, however, may promote a higher corrosion rate. Alternatively, a metal such as Sn or Cd, may be chosen based on their low exchange current density so as not to promote corrosion reactions. Thus, in the case of Sn or Cd layers both hydrogen absorption and corrosion are reduced by the barrier and by the inhibiting nature of the coating surface for the h.e.r., respectively.

EXPERIMENTAL

A Devanathan and Stachurski cell [17] was used to measure the permeability of hydrogen through coated Ferrovac E iron membranes. It consists of two identical electrolytic cells separated by the metal membrane. Cell 1 and associated circuitry is used to generate the hydrogen charging current and to measure the potential of the charging side, while cell 2, is used to monitor the flux of hydrogen diffusing through the membrane by measuring the hydrogen oxidation current at its pallidized exit surface. The electrode potential at the exit surface is sufficiently positive to oxidize all of the

hydrogen arriving at the surface [1]. The reference electrodes were Hg/HgO and the measured potentials were converted to, and reported on, the standard hydrogen electrode (SHE) scale. The charging solution in cell 1 was 0.1N NaOH + 2ppm As while cell 2 was filled with 0.1N NaOH. The Ferrovac E iron membranes (0.037 cm thick) were polished down to 600 emery paper and annealed in an evacuated capsule which had been purged with an Ar-1% H₂ gas mixture at 1000°C for 2 hrs. Details of the membrane preparation, cell design, circuitry, the potential at the exit side of the membrane, edge effects, proper membrane thickness...etc. are presented elsewhere [1].

The experimental technique was essentially that commonly used in studying the kinetics of the hydrogen evolution reaction. Strict conditions of purity and deaeration were maintained throughout the measurements. The solutions were pre-electrolyzed overnight under an atmosphere of prepurified nitrogen using a Pt anode which was separated from the solution by a glass frit and and Fe cathode, and then transferred from the pre-electrolysis cell to the permeation cell under nitrogen. The measurements were taken galvanostatically in both the ascending and descending directions. The charging current was changed in steps. The potential was recorded after a stationary value was obtained, usually after 2-3 minutes. All measurements were taken at 25±3°C.

Cadmium was electrodeposited at room temperature from a cyanide bath [18] (25gm l⁻¹ CdO, 75 gm l⁻¹ NaCN and 15 gm l⁻¹ NaOH) by a strike of 100 mA cm⁻² at room temperature from a sodium stannate bath containing 100 gm l⁻¹ Na₂SnO₃, 10 gm l⁻¹ NaOH, 15 gm l⁻¹ CH₃COONa and 10 ml l⁻¹ of 3% H₂O₂ [19]. The current efficiencies of these baths were determined by coulometric, weight gain, and thickness analyses, and their continuity was determined by SEM cross-section and topographic examinations. X-ray diffraction examination confirmed that the lattice parameters and crystallographic structures were those of Cd and β-Sn.

In order to obtain reproductibility of the permeation data several different precharging procedures were evaluated. The procedure adopted consists of precharging the uncoated iron membrane in 0.1N NaOH for about 45 minutes at 10 mA cm^{-2} prior to a permeation measurement in 0.1N NaOH solution containing 2 ppm As. A coating of specified thickness was then applied in situ after draining and refilling the cell with the plating solution. Following this step the cell was drained, thoroughly washed with doubly distilled water and filled again with fresh 0.1N NaOH containing 2 ppm As for permeation runs on the coated iron membrane. Permeation data on thicker coatings were obtained by repeating these steps. All solutions were changed under a N_2 atmosphere. Arsenic was added to the charging solution because in its absence no hydrogen was found to diffuse through the coated iron. Arsenic has the effect of increasing the kinetics of hydrogen entry into iron [20]. Cross-section examination of the membranes following the permeation experiment included preparation of the cross section by fracturing the membrane in liquid nitrogen.

RESULTS

Figs. 2 and 3 show the cross section and surface morphologies of the Sn and Cd electrodeposits. Porosity is a factor for both metals; in the case of Cd a more dense layer forms under the outer deposit. In cooling to liquid nitrogen temperature the room temperature stable β -Sn phase may have transformed to the stable low temperature α -Sn and then transformed back again to β -Sn on returning to room temperature. The liquid nitrogen step, however, had no effect on the morphology of the Sn, Fig. 2.

Fig. 4 shows the dependency of hydrogen absorption on Cd and Sn plating time for a deposition current density of 1 mA cm^{-2} . The total time of plating for cadmium corresponds to a 3- μm thick coat and for Sn to a 1.5- μm thick coat.

The measured electrode potential during Cd deposition drifted slightly (0.03V) in the less noble direction to a final value of -1.1V (S.H.E.), and during Sn deposition drifted about 0.3V to a final value of -1.6V. The transients show that the maximum permeation currents are $15.6 \mu\text{A cm}^{-2}$ (1×10^{14} atoms $\text{H cm}^{-2} \text{s}^{-1}$) for cadmium and $21.2 \mu\text{A cm}^{-2}$ (1.3×10^{14} atoms $\text{H cm}^{-2} \text{s}^{-1}$) which correspond to 6 nm (60 Å) and 130 nm thick coats for plating times of 27 sec and 3.35 min., respectively.

Fig. 5 shows a typical permeation transient for hydrogen permeation through uncoated iron. It also shows the effect of Cd and Sn coats (of different thickness) on the permeation transient of hydrogen through the coated iron membrane. At comparable thickness, Sn gives the lower permeability. It is also clear that the hydrogen permeation flux decreases as the coating thickness increases for both Cd and Sn. The measured electrode potential during hydrogen charging at a fixed impressed cathodic current was always considerably less noble on the coated membranes than on the uncoated Fe membrane (Fig. 6). Tafel behavior is observed for the coated and uncoated membranes, Fig. 6.

Fig. 7 shows the (quasi) steady-state permeation current as a function of the reciprocal of the coating thickness for Cd and Sn. The results for Cd at both charging currents and for Sn at the two higher charging currents satisfactorily fit straight line relations passing through the origin (infinite coating thickness). This indicates, as discussed below, that the permeation process was controlled by diffusion through the coatings.

Table 1 lists the values of DC° and C° for both Cd and Sn coatings for different charging currents. The quantity C° is the hydrogen solubility just inside the metal surface at the overpotential considered [21]. Table 1 includes a column for the electrode potential at the charging surface of the membrane, since the latter is the driving force for the hydrogen evolution reaction and,

hence, also for the hydrogen absorption process. The solubility C° is an important quantity with regard to avoiding mechanical degradation of steel. The C° values are lower for Sn-coated than for Cd-coated iron, Table 1.

Table 2 lists the diffusivity values obtained for Cd and Sn coated iron membranes from the rise and decay time of the permeation transients [21]. In obtaining D, the experimentally determined thickness of the respective coating was used without correction for porosity; the true D is smaller in proportion to the ratio of the effective-to-measured thickness, estimated at 2 to 5 times.

DISCUSSION

The Tafel line on the uncoated Fe membrane (Fig 6) is in agreement with those obtained previously [22]. The potential shifts shown in Fig. 6 indicated that the h.e.r. is more facile on Fe than on Cd than on Sn. This result is compatible with the finding [23,24] that the efficiency of these metals in catalyzing the rate of combination of absorbed hydrogen is in the order $\text{Fe} > \text{Cd} > \text{Sn}$.

During the electrodeposition step, the permeation current, prior to growth of the deposit to a thickness giving significant barrier character, is quite high, e.g., the maximum values in Fig. 4, especially compared to permeation rates for As-free sodium hydroxide charging solutions, i.e., $\sim 3 \mu\text{A cm}^{-2}$ [25]. These results support the findings that compounds of CN^- in electroplating baths increase the absorption [21,26] and, consequently, the embrittling influence of hydrogen. The large hydrogen permeation during Sn plating also is consistent with the observation that high-strength steel is highly embrittled when plated with tin from the alkaline stannate bath [27]. The large hydrogen absorption, in this case, is attributed to the stannate ion.

The permeation transients obtained during electrodeposition (Fig. 4) Show

Table 1. DC° , C° and electrode potential at different hydrogen charging current densities in 0.1N NaOH + 2ppm As^{+3} for Sn and Cd coatings of Fe.

i $mA\ cm^{-2}$	$DC^\circ \times 10^{15}$ $g\text{-atom}\ cm^{-1}\ s^{-1}$	$C^\circ \times 10^5$ $g\text{-atom}\ cm^{-3}$	$-E, V, (SHE)$					
			Sn			Cd		
			Coating Thickness μm			Coating Thickness		
			1.0	1.67	3.0	1.12	3.0	6.0
0.127	1.0	13.0	1.325	1.352	1.370	1.273	1.329	1.432
0.254	1.4	17.5	1.418	1.472	1.491	1.344	1.413	1.471
0.381	1.5	--	1.474	1.530	1.559	--	--	--
0.636	--	26.5	--	--	--	1.418	1.497	1.518
0.890	2.4	--	1.572	1.653	1.687	--	--	--
1.27	2.9	34.0	1.597	1.702	1.723	1.476	1.559	1.559
2.54	3.6	40.0	1.682	1.758	1.830	1.533	1.618	1.605
5.09	4.6	--	1.749	1.821	1.829	--	--	--

that during an initial period hydrogen permeation increases in the normal way. During this period, the rates of hydrogen evolution and absorption are dependent, seemingly to a high degree, on the availability of the iron surface. This is to be expected since both the catalytic nature of Sn and Cd for the hydrogen evolution reaction and the permeability of H in Sn and Cd are lower than in the case of iron. In the second stage, for both metals there is a marked reduction in hydrogen absorption (permeation) with time of plating, consistent with the formation of a continuous and sufficiently thick electrodeposit which then functions as a good barrier to hydrogen. Though these effects are similar for both Cd and Sn, the time frame is quite long during Sn plating so that the maximum permeation rate is reached only after the deposit thickness on average reaches $\sim 0.13 \mu\text{m}$. This is consistent with the quite porous nature of the Sn coat evident in Fig. 2, so that a relatively large amount of deposition occurs prior to the establishment of a continuous layer which functions as a barrier to hydrogen permeation. The shorter time during Cd plating indicates that a dense layer forms more quickly, during or preceding formation of an outer porous layer consisting of weakly bound, large scale crystallinities, Fig. 3.

It is well known that hydrogen embrittlement is, among other factors, a function of the total amount of hydrogen travelling in and across the plate [21,28]. The area under the permeation-time transient between time on, and time off, of the charging current is a measure of the total amount of hydrogen introduced into the system. The permeation data obtained during electrodeposition indicates that the Cd plating bath introduces less hydrogen into the Fe membrane than does the Sn plating bath for comparable plating thickness. This occurs in spite of the higher permeability of cadmium (Fig. 5) and is, therefore, concluded to be simply due to the faster build up of a continuous Cd deposit (Fig. 4) and a lower hydrogen evolution rate (higher efficiency of the Cd bath). The

Table 2. Values of hydrogen diffusivity through Sn and Cd coatings based on coating thickness without correction for porosity.

Metal	Diffusion Coefficient, $\text{cm}^2 \text{s}^{-1}$ @ 25°C		
	Rise Time	Decay Time	Average
Sn	3.2×10^{-10}	4.6×10^{-10}	4.0×10^{-10}
Cd	4.6×10^{-10}	4.6×10^{-10}	4.6×10^{-10}

latter is consistent with cadmium's more noble electrode potential during deposition.

The slope of each of the plots in Fig. 7 is $\partial i_{\infty} / \partial (1/L) = FD [C^{\circ} - C_{M-Fe}]$, where C° and C_{M-Fe} are the concentrations of hydrogen in the lattice at the outer surface of the coating and at the phase boundary between the coating and the iron substrate, respectively; F is the Faraday constant; and L is the thickness of the coating. When diffusion through the coating is rate determining it follows that the permeation process is relatively fast through the iron membrane, and hence, C_{M-Fe} approaches the value at the exit side of the (iron) membrane, i.e., $C_{M-Fe} \rightarrow 0$. Thus, the slope becomes equal to FDC° , for which the plot of i_{∞} vs. $1/L$ yields a straight line passing through the origin. A large slope indicates a large value of the product DC° , i.e., a large diffusivity and/or concentration and obviously a less effective coating. Such data indicate that the hydrogen solubility just inside the coating surface for tin-plated iron is less than that for cadmium-plated iron. Thus, in contrast to the situation during the electrodeposition step, there will be less embrittling influence of hydrogen during hydrogen charging of Sn-coated, than of Cd-coated iron.

CONCLUSIONS

1. Sn and Cd electrodeposits on iron are shown to be effective barriers to hydrogen at thicknesses $\geq 1 \mu m$. By controlling electroplating conditions to reduce porosity, even thinner coatings have the potential to be effective barriers.
2. The diffusivity of hydrogen was determined to be on the order of $10^{-10} \text{ cm}^2 \text{ s}^{-1}$ at 25°C in both Sn and Cd.
3. A modification of the permeation method (use of a bilayer, rather than single layer membrane) extends the range of diffusivity which can be readily measured to much lower values.

4. It is shown that, in principle, the nature of the coating surface with regard to promoting the h.e.r. can strongly affect hydrogen absorption. As such a new method of controlling hydrogen absorption is presented.

ACKNOWLEDGEMENTS

Mr. R. Hafley and Mr. D. R. Marx provide technical assistance. Sponsorship by the Metallurgy Branch of the Office of Naval Research, under contract N000-14-75-C-0264 is gratefully acknowledged.

REFERENCES

1. S. S. Chatterjee, B. G. Ateya and H. W. Pickering, Met. Trans 9A, 389-95 (1978).
2. H. W. Pickering and M. Zamanzadeh, Proc. Third Intern. Conf. on Effect of Hydrogen on Behavior of Materials, I. M. Bernstein and A. W. Thompson, ed; TMS-AIME, New York, to be published.
3. M. Zamanzadeh, A. Allam, H. W. Pickering and G. K. Hubler, J. Electrochem. Soc., 127, 1688 (1980).
4. E. Enyo, Electrochem Acta, 18, 155 (1973).
5. J. O'M. Bockris and P. K. Subramanyan, Electrochem Acta, 16, 2169-2179 (1971).
6. R. Brunetard, R. Chevalier, and R. Martinov, L'Hydrogene dans les Metaux', Valduc, 83 (1969).
7. E. Kunze, Second International Congress on Hydrogen in Metals, Paris, France, 6A5 (1977).
8. V. I. Baranovsky, V. T. Stepurenko, and M. G. Sakharov, Fiz-Khim Mekhan. Mat., 8, 15 (1972).
9. C. F. Barth and A. R. Troiano, Corrosion, 2B, 259 (1972).
10. A. R. Troiano, Corrosion, 15, 207 t (1959).
11. W. I. Cotton, Plating, 2, 169 (1960).
12. M. A. V. Devanathan and Z. Stachurski, J. Electrochem Soc. 110, 887 (1963).
13. V. N. Kudoyavtsev, K. S. Pedan, N. K. Baraboshkina and A. T. Vagramyan, Trans IMF, 50, 223 (1972).
14. W. Roger Buck, III, and Henry Leidheiser, Jr., J. Electrochem. Soc., 112, 243 (1965).
15. V. I. Zhitenev, V. Z. Strizkak, L. P. Sereckina, V. P. Levehenko and R. A. Rvabov, Zashchita Metallov, 10, 462-463 (1974).
16. M. A. Figelman and A. V. Shreider, J. Appl. Chem (USSR), 31, 1175 (1958).
17. M. A. V. Devanathan and Z. Stachurski, Proc. Roy. Soc. A270, 90 (1962).
18. A. E. Yaniv, T. P. Radhakrishnan and L. L. Shreir, Trans. Inst. Met. Finish., 45, pp. 1-9 (1967).
19. F. A. Lowenheim, Modern Electroplating, John Wiley and Sons, New York (1974).

20. T. Zakroczymski, Z. Szklarska Smialowska and M. Smialowski, *Werkstoffe und Korrosion*, 26, 617 (1975).
21. J. O'M. Bockris, Proceedings of International Conference on Stress Corrosion Cracking and Hydrogen Embrittlement of Iron Base Alloys, Firminy, France, P. 287, June 1973.
22. J. O'M. Bockris, J. McBreen, and L. Nanis, *J. Electrochem Soc.*, 112, 1025 (1965).
23. G. G. Bond, *Catalysis by Metals*, Academic Press, P. 176, (1962).
24. T. Erdey-Gruz, *Kinetics of Electrode Process*, Wiley Interscience, New York, 164 (1972).
25. M. Zamanzadeh and H. W. Pickering, unpublished data.
26. W. Beck and J. E. Jankowsky, *Proc. Am. Electroplaters Soc.*, 47, 152 (1960).
27. H. J. Read, *Hydrogen Embrittlement in Metal Finishing*, New York, 161 (1961).
28. H. P. Tadrif and H. Marquis, *Can. Metal. Quart.*, 1, 153, (1962).

FIGURE CAPTIONS

- Figure 1 Relative polarization behavior for hydrogen evolution on a deposit (2) and on a substrate (1) for the condition $(i_o)_2 \gg (i_o)_1$. Note that $\eta_{1,2}$ (sketch at left) is much than η_1 for the deposit-free substrate during hydrogen charging at a give rate, I.
- Figure 2 SEM micrographs of a cross section (top) and the surface of a Sn electrodeposit on Fe. Cross section was obtained by fracturing in liquid N_2 . S_n , S_n^x and Fe_x are Sn surface, Sn cross section and Fe cross section, respectively.
- Figure 3 SEM micrographs as in Fig. 2, but of a Cd electrodeposit.
- Figure 4 Hydrogen permeation through Fe membranes during electrodeposition of Sn or Cd onto the Fe_2 surface. Deposition current for both Sn and Cd was 1 mA cm^{-2} .
- Figure 5 Effect of Sn and Cd-coating thickness on hydrogen permeation through a Ferrovac- E iron membrane (0.37 mm thick). Charging current was 0.25 mA cm^{-2} . Charging solution was $0.1N \text{ NaOH} + 2 \text{ ppm As}^{3+}$.
- Figure 6 Tafel plots for hydrogen evolution on Fe, and on Sn and Cd-coated Fe membranes.
- Figure 7 Dependence of the steady-state hydrogen permeation current on the reciprocal of the thickness of the Cd and Sn coats.

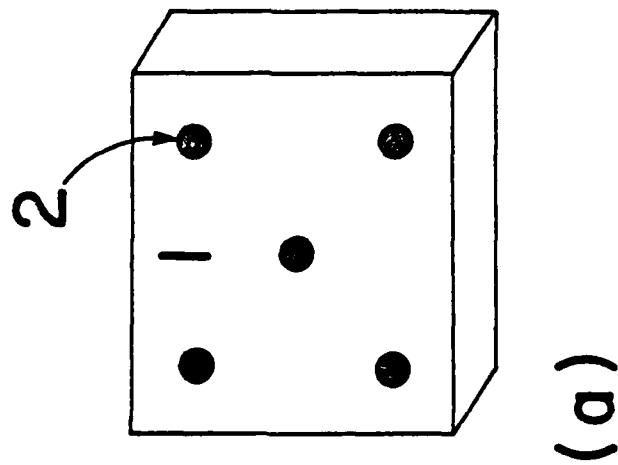
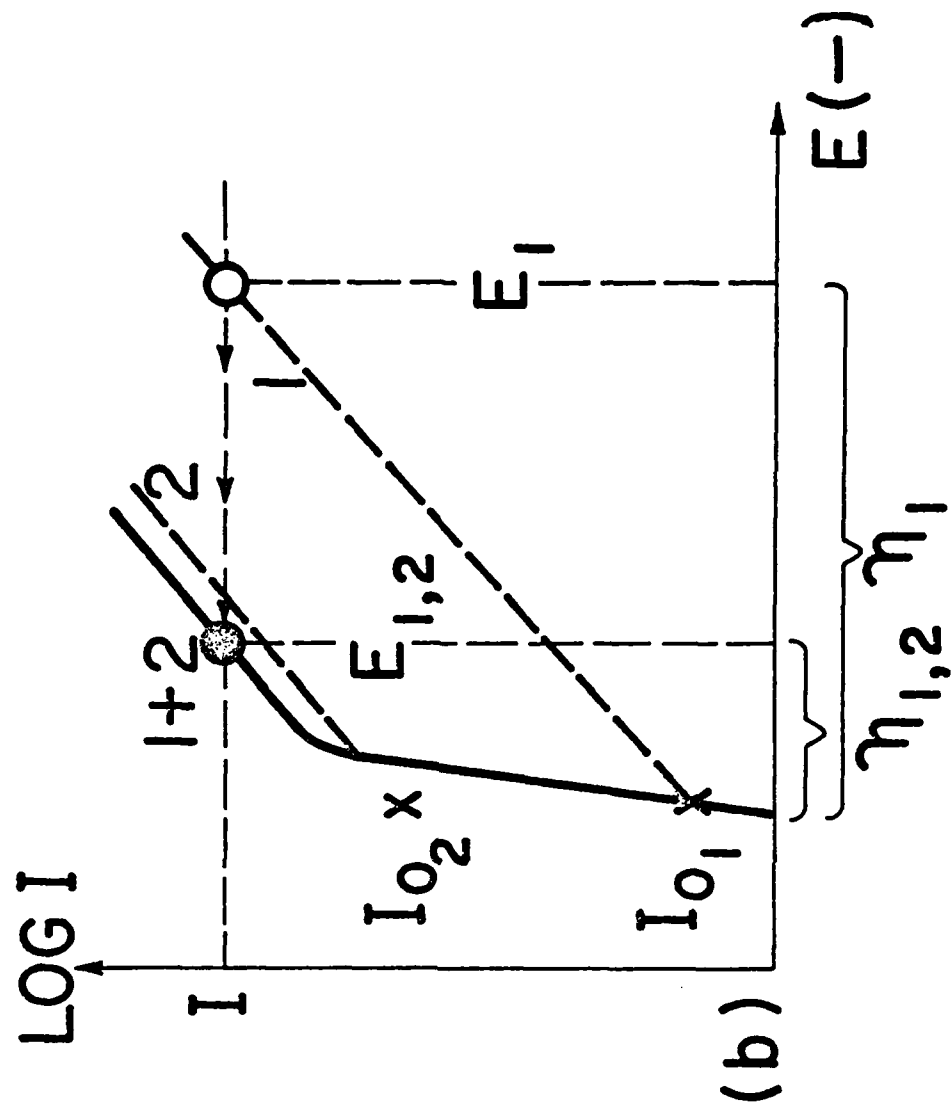


Figure 1

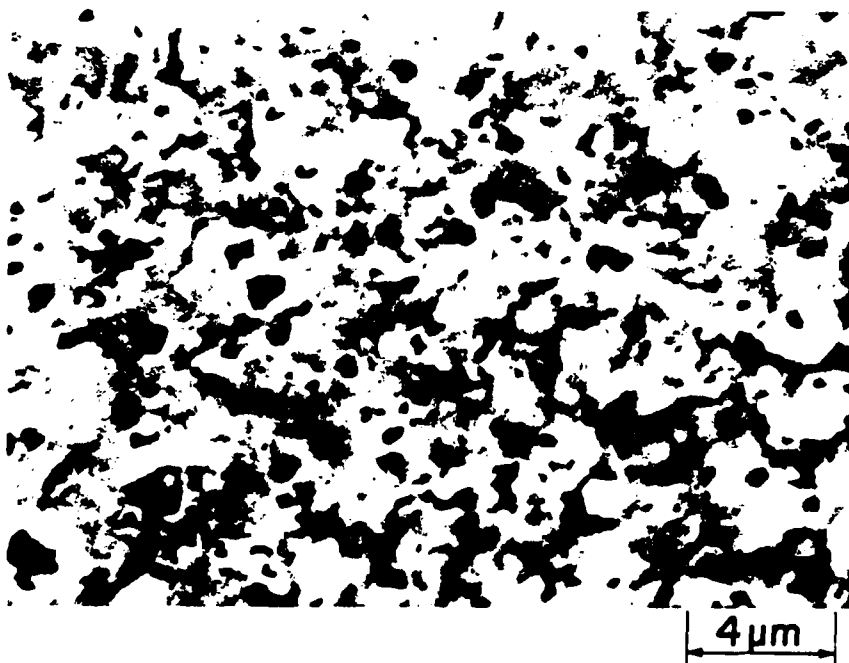
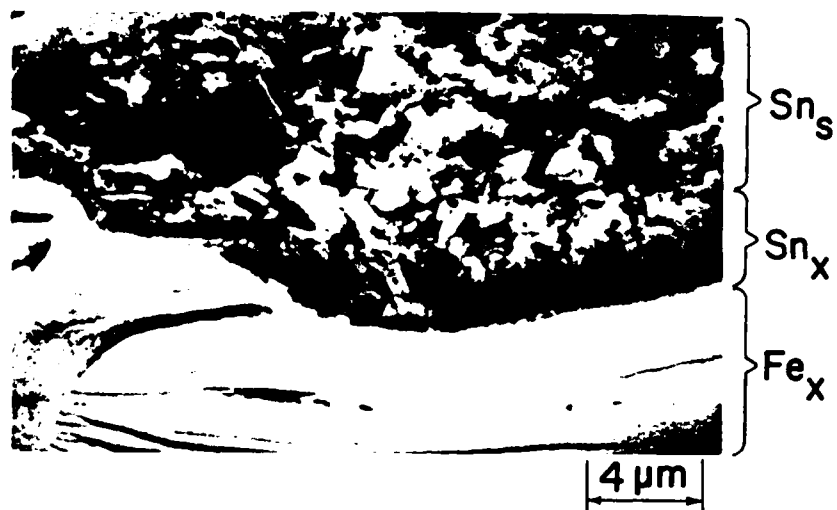


Figure 2

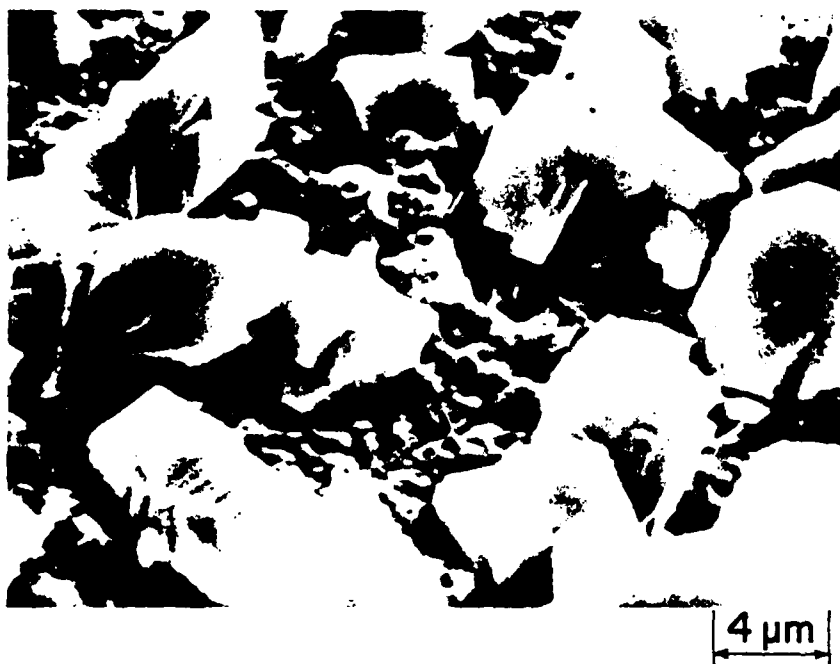
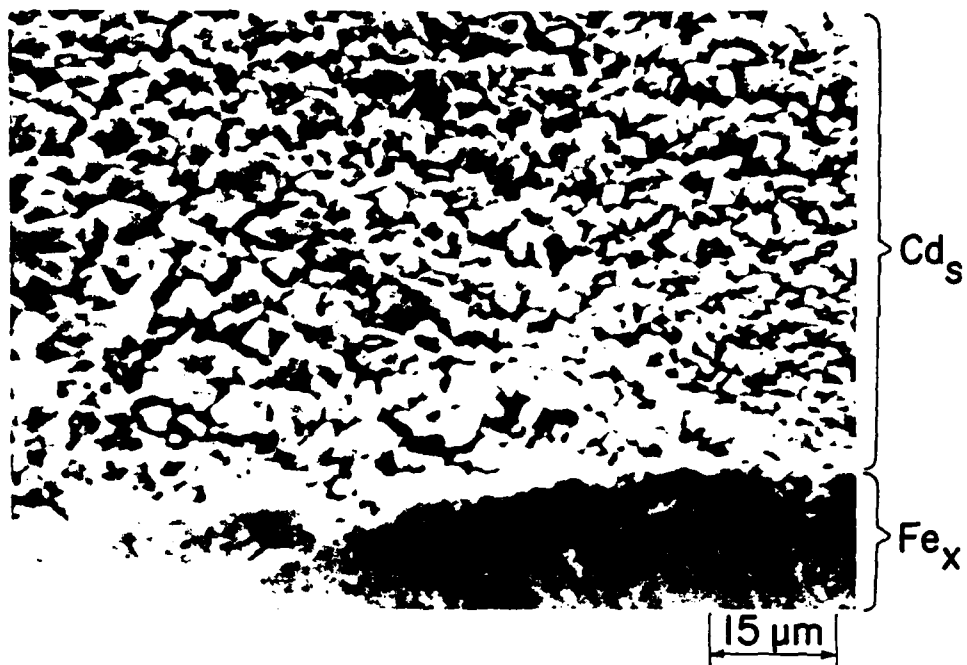


Figure 3

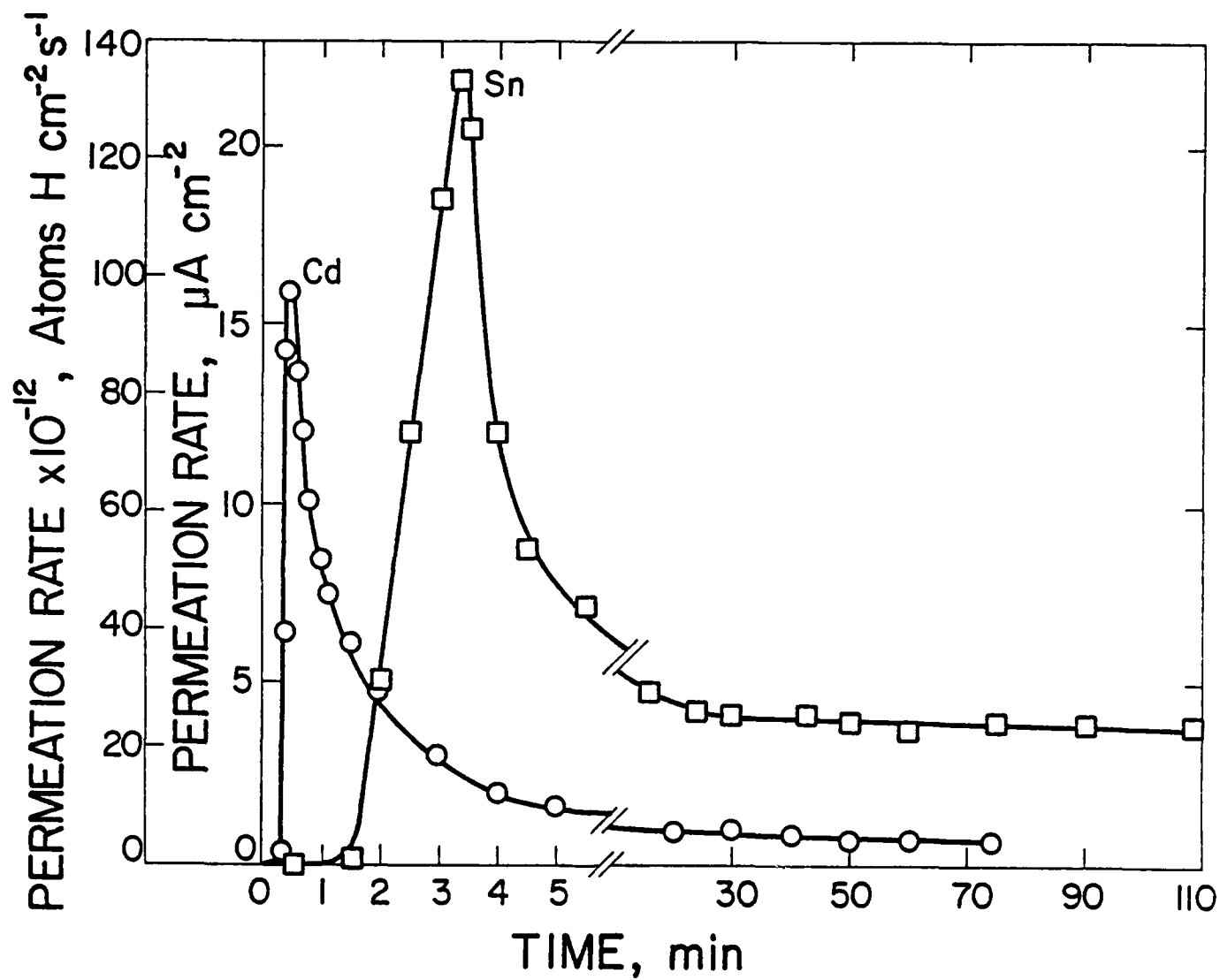


Figure 4

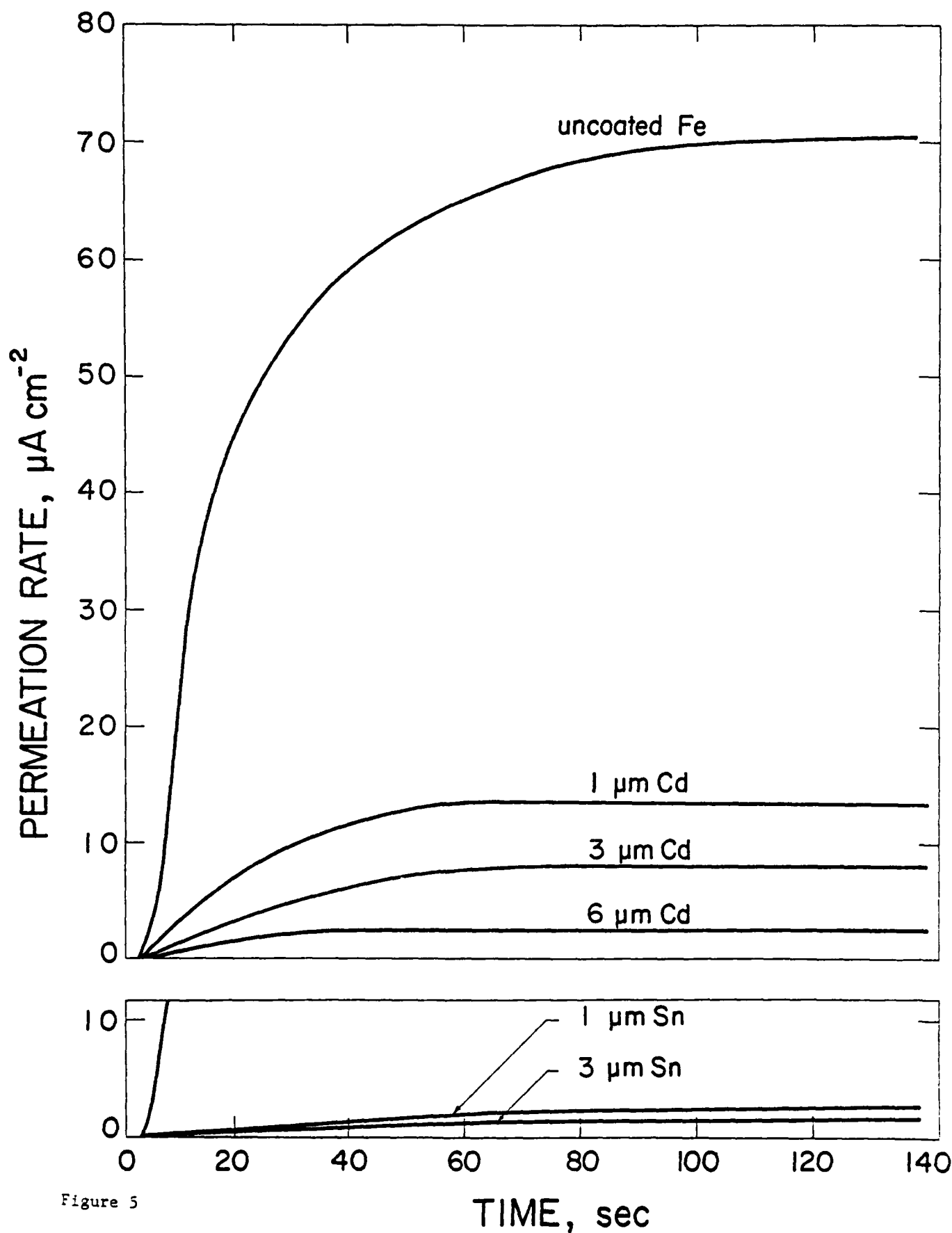


Figure 5

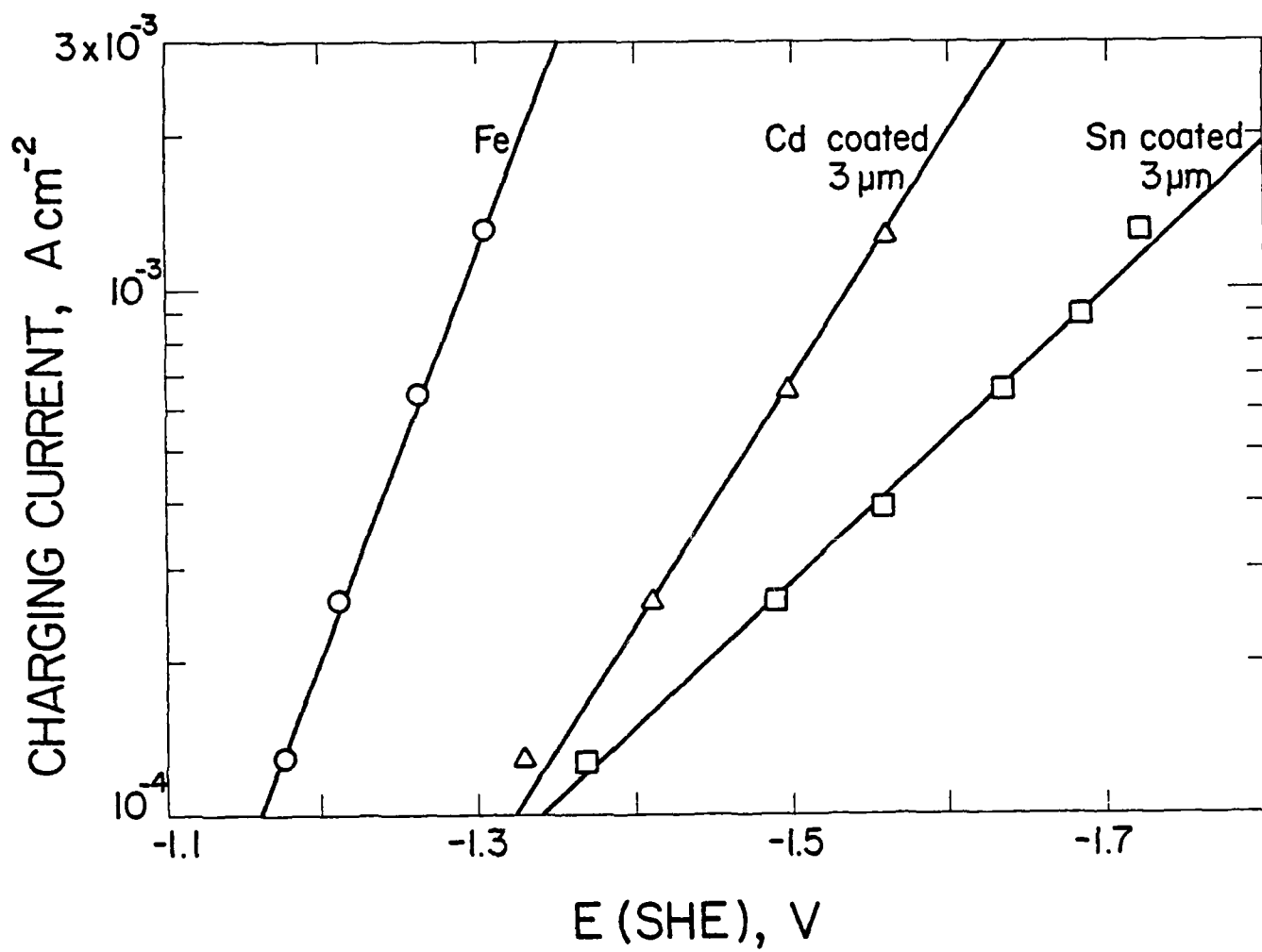
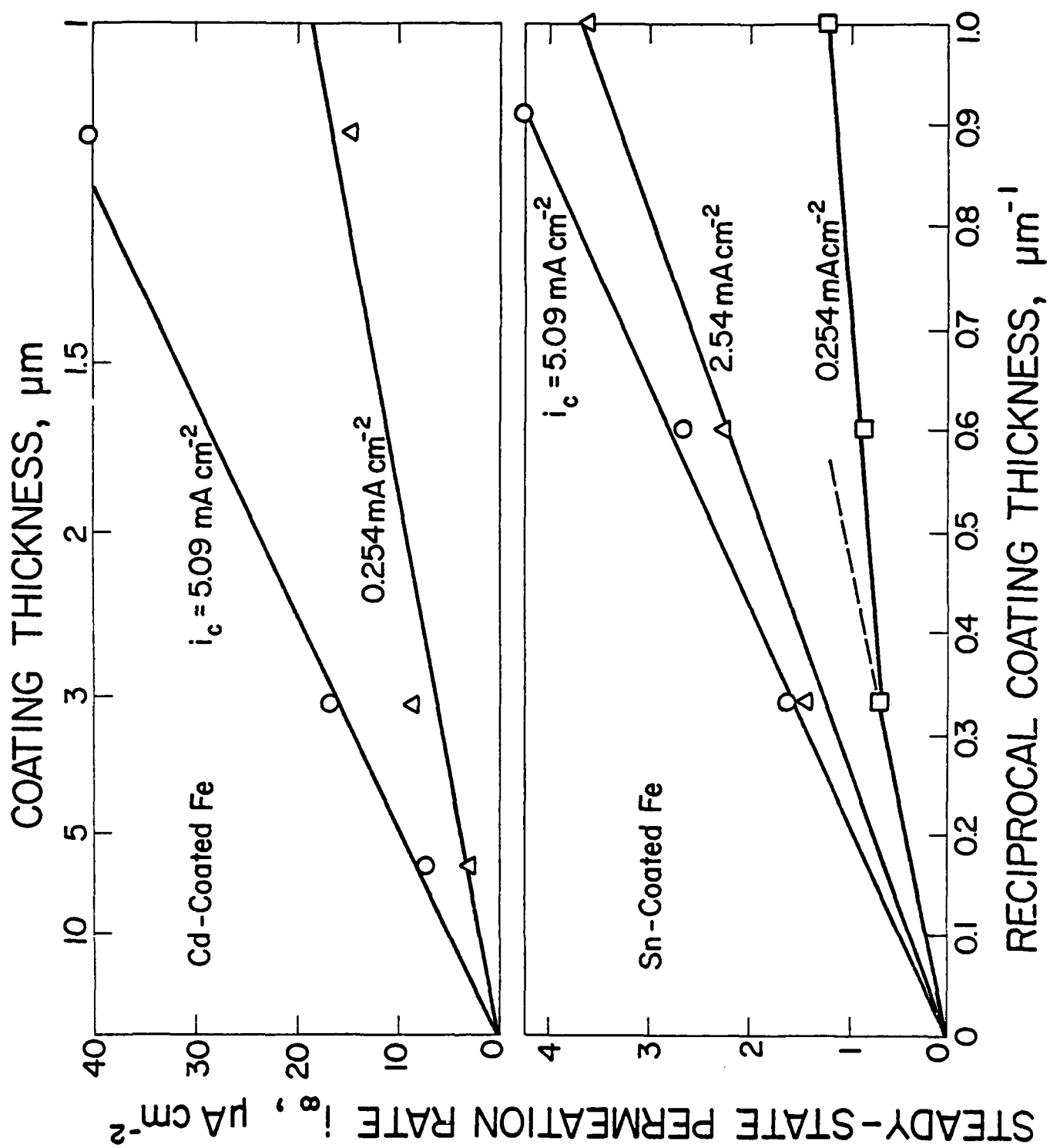


Figure 6

Figure 7



BASIC DISTRIBUTION LIST

Technical and Summary Reports

November 1979

<u>Organization</u>	<u>Copies</u>	<u>Organization</u>	<u>Copies</u>
Defense Documentation Center Cameron Station Alexandria, VA 22314	12	Naval Air Propulsion Test Center Trenton, NJ 08628 ATTN: Library	1
Office of Naval Research Department of the Navy 800 N. Quincy Street Arlington, VA 22217 ATTN: Code 471 Code 470	1 1	Naval Construction Battalion Civil Engineering Laboratory Port Hueneme, CA 93043 ATTN: Materials Division	1
Commanding Officer Office of Naval Research Branch Office Building 114, Section D 666 Summer Street Boston, MA 02210	1	Naval Electronics Laboratory San Diego, CA 92152 ATTN: Electron Materials Sciences Division	1
Commanding Officer Office of Naval Research Branch Office 536 South Clark Street Chicago, IL 60605	1	Naval Missile Center Materials Consultant Code 3312-1 Point Mugu, CA 92041	1
Naval Research Laboratory Washington, DC 20375 ATTN: Codes 6000 6100 6300 2627	1 1 1 1	Commanding Officer Naval Surface Weapons Center White Oak Laboratory Silver Spring, MD 20910 ATTN: Library	1
Naval Air Development Center Code 606 Warminster, PA 18974 ATTN: Dr. J. Deluccia	1	Commander David W. Taylor Naval Ship Research and Development Center Bethesda, MD 20084	1
		Naval Oceans Systems Center San Diego, CA 92132 ATTN: Library	1
		Naval Underwater System Center Newport, RI 02840 ATTN: Library	1
		Naval Postgraduate School Monterey, CA 93940 ATTN: Mechanical Engineering Department	1
		Naval Weapons Center China Lake, CA 93555 ATTN: Library	1

BASIC DISTRIBUTION LIST (cont'd)

<u>Organization</u>	<u>Copies</u>	<u>Organization</u>	<u>Copies</u>
Naval Air Systems Command Washington, DC 20360 ATTN: Codes 52031 52032	1 1	NASA Lewis Research Center Lewis Research Center 21000 Brookpark Road Cleveland, OH 44135 ATTN: Library	
Naval Sea System Command Washington, DC 20362 ATTN: Code 05R	1	National Bureau of Standards Washington, DC 20234 ATTN: Metals Science and Standards Division Ceramics Glass and Solid State Science Division Fracture and Deformation Division	
Naval Facilities Engineering Command Alexandria, VA 22331 ATTN: Code 03	1	Director Applied Physics Laboratory University of Washington 1013 Northeast Forthieth Street Seattle, WA 98105	
Scientific Advisor Commandant of the Marine Corps Washington, DC 20380 ATTN: Code AX	1	Defense Metals and Ceramics Information Center Battelle Memorial Institute 505 King Avenue Columbus, OH 43201	
Army Research Office P.O. Box 12211 Triangle Park, NC 27709 ATTN: Metallurgy & Ceramics Program	1	Metals and Ceramics Division Oak Ridge National Laboratory P.O. Box X Oak Ridge, TN 37380	
Army Materials and Mechanics Research Center Watertown, MA 02172 ATTN: Research Programs Office		Los Alamos Scientific Laboratory P.O. Box 1663 Los Alamos, NM 87544 ATTN: Report Librarian	1
Air Force Office of Scientific Research/NE Building 410 Bolling Air Force Base Washington, DC 20332 ATTN: Chemical Science Directorate Electronics & Materials Sciences Directorate	1 1	Argonne National Laboratory Metallurgy Division P.O. Box 229 Lemont, IL 60439	1
Air Force Materials Laboratory Wright-Patterson AFB Dayton, OH 45433	1	Brookhaven National Laboratory Technical Information Division Upton, Long Island New York 11973 ATTN: Research Library	1
Library Building 50, Room 134 Lawrence Radiation Laboratory Berkeley, CA 94700		Office of Naval Research Branch Office 1030 East Green Street Pasadena, CA 91106	1
NASA Headquarters Washington, DC 20546 ATTN: Code RRM	1		

Sept 1980

SUPPLEMENTARY DISTRIBUTION LIST

Technical and Summary Reports

Dr. T. R. Beck
Electrochemical Technology Corporation
10035 31st Avenue, NE
Seattle, Washington 98125

Professor I. M. Bernstein
Carnegie-Mellon University
Schenley Park
Pittsburgh, Pennsylvania 15213

Professor H. K. Birnbaum
University of Illinois
Department of Metallurgy
Urbana, Illinois 61801

Dr. Otto Buck
Rockwell International
1049 Camino Dos Rios
P.O. Box 1085
Thousand Oaks, California 91360

Dr. W. Morris
Rockwell International
1049 Camino Dos Rios
P.O. Box 1085
Thousand Oaks, California 91360

Dr. David L. Davidson
Southwest Research Institute
600 Culebra Road
P.O. Drawer 28510
San Antonio, Texas 78284

Dr. D. J. Duquette
Department of Metallurgical Engineering
Rensselaer Polytechnic Institute
Troy, New York 12181

Professor R. T. Foley
The American University
Department of Chemistry
Washington, D. C. 20016

Dr. J. A. S. Green
Martin Marietta Corporation
1450 South Rolling Road
Baltimore, Maryland 21227

Professor R. H. Heidersbach
University of Rhode Island
Department of Ocean Engineering
Kingston, Rhode Island 02881

Professor H. Herman
State University of New York
Material Sciences Division
Stony Brook, New York 11970

Professor J. P. Hirth
Ohio State University
Metallurgical Engineering
1314 Kinnear Road
Columbus, Ohio 43212

Professor R. M. Latanision
Massachusetts Institute of Technology
77 Massachusetts Avenue
Room E19-702
Cambridge, Massachusetts 02139

Dr. F. Mansfeld
Rockwell International Science Center
1049 Camino Dos Rios
P.O. Box 1085
Thousand Oaks, California 91360

Dr. Jeff Perkins
Naval Postgraduate School
Monterey, California 93940

Dr. E. A. Starke, Jr.
Georgia Institute of Technology
School of Chemical Engineering
Atlanta, Georgia 30332

Dr. R. P. Wei
Lehigh University
Institute for Fracture and
Solid Mechanics
Bethlehem, PA 18015

SUPPLEMENTARY DISTRIBUTION LIST (continued)

Professor H. G. F. Wilsdorf
University of Virginia
Department of Materials Science
Charlottesville, Virginia 22903

Dr. Clive Clayton
State University of New York
Material Sciences Division
Stony Brook, New York 11970

Dr. Henry Leidheiser
Center for Surface and Coatings Research
Sinclair Memorial Laboratory 7
Lehigh University
Bethlehem, PA 18015

SECURITY CLASSIFICATION OF THIS PAGE (When Data Entered)

(14) TR-16


REPORT DOCUMENTATION PAGE		READ INSTRUCTIONS BEFORE COMPLETING FORM
1. REPORT NUMBER Technical Report No. 15	2. GOVT ACCESSION NO. AD-A096309	3. RECIPIENT'S CATALOG NUMBER
4. TITLE (and Subtitle) Hydrogen Absorption During Electrodeposition and Hydrogen Charging of Sn and Cd Coatings on Iron.		5. TYPE OF REPORT & PERIOD COVERED Technical Progress Report
6. AUTHOR(s) M./Zamanzadeh, A./Allam, C./Kato, B./Ateya and H. W./Pickering		7. PERFORMING ORG. REPORT NUMBER
8. PERFORMING ORGANIZATION NAME AND ADDRESS Metallurgy Section, 209 Steidle Building The Pennsylvania State University University Park, PA 16802		9. CONTRACT OR GRANT NUMBER(s) N00014-75-C-0264
10. CONTROLLING OFFICE NAME AND ADDRESS Metallurgy Branch Office of Naval Research Arlington, VA 22217		11. PROGRAM ELEMENT, PROJECT, TASK AREA & WORK UNIT NUMBERS
12. MONITORING AGENCY NAME & ADDRESS (if different from Controlling Office) 12 35		13. REPORT DATE February 1981
		14. NUMBER OF PAGES 23
		15. SECURITY CLASS. (of this report)
		15a. DECLASSIFICATION/DOWNGRADING SCHEDULE
16. DISTRIBUTION STATEMENT (of this Report) Distribution of this document is unlimited		
17. DISTRIBUTION STATEMENT (of the abstract entered in Block 20, if different from Report)		
18. SUPPLEMENTARY NOTES		
19. KEY WORDS (Continue on reverse side if necessary and identify by block number) Hydrogen embrittlement, Electroplating, Hydrogen catalysts, H Diffusivity and solubility.		
20. ABSTRACT (Continue on reverse side if necessary and identify by block number) A study was made of the extent of hydrogen absorption during electrodeposition of Sn or Cd onto an Fe Substrate, and, subsequently during electrolytic hydrogen charging of the Sn or Cd-coated Fe membranes. The effectiveness of deposits, in general, for decreasing hydrogen absorption by the substrate is discussed in terms of their barrier character and of their catalytic nature for promoting the hydrogen evolution reaction. The latter is a new method for decreasing hydrogen absorption. The reduction in hydrogen absorption was found to be in		

DD FORM 1 JAN 73 1473

EDITION OF 1 NOV 65 IS OBSOLETE
S/N 0102-LF-014-6601

SECURITY CLASSIFICATION OF THIS PAGE (When Data Entered)

4104352

proportion to the coating thickness at $\geq 1 \mu\text{m}$. Analysis of the data indicates that diffusion of hydrogen through the coating is the rate determining step of the permeation process, and that the product of the diffusivity and solubility of hydrogen is in the following order: $\text{Sn} < \text{Cd} < \text{Fe}$. The effective diffusivity of hydrogen at 25°C in both the Sn and Cd electrodeposits $\approx 10^{-10} \text{ cm}^2\text{s}^{-1}$. These diffusivities could be obtained in relatively short time experiments since the coatings were quite thin. As such the bilayer membrane offers advantages over the usual single layer membrane for obtaining the diffusivity of hydrogen in metals for which the permeability is very low. 

1. $10^{-10} < 10^{-11}$ cm²s⁻¹
2. $10^{-11} < 10^{-12}$ cm²s⁻¹

DATE
FILMED
-8